Al-Khwarizmi Engineering Journal
ISSN (printed): 1818 – 1171, ISSN (online): 2312 – 0789
Vol. 22, No. 1, March, (2026), pp. 127- 151

Al-Khwarizmi Engineering Journal

Comparative Analysis of Different Imaging Techniques for Measuring the Neck–Shaft Angle in the Proximal Femur

Sajjad Abbas Ali[1]*, Ahmed Z.M. Shammari[2], and Wamieth A.J. Augla[3]
[1,2] *Department of Automated Manufacturing Engineering, Al-Khwarizmi College of Engineering, University of Baghdad, Baghdad, Iraq*
[3] *Orthopaedic Surgeon, Yarmouk Teaching Hospital, Ministry of Health, Baghdad, Iraq*
*Corresponding Author's Email: sajjad.ali2204@kecbu.uobaghdad.edu.iq

(Received 25 June 2024; Revised 25 January 2025; Accepted 6 April 2025; Published 1 March 2026)
https://doi.org/10.22153/kej.2026.04.001

Abstract

Clinical settings have an accurate neck–shaft angle (NSA) because it directly affects the diagnosis and treatment of hip-related conditions such as hip dysplasia and osteoarthritis. Variations in NSA measurement can lead to a difference in the patient's condition during imaging and emphasize the importance of standardized protocols to ensure reliability. Reducing measurement anomalies enables health professionals to improve surgical planning and patient results significantly. A functioning method and its effect on clinical applications to evaluate different imaging techniques and software platforms based on correlation coefficients in the class can be used to determine stability and reliability. The primary goal of this research is to identify a valid, reliable NSA measurement using different software and methods. The final results indicate that the 3D method for measuring NSA, primarily using artificial-intelligence-driven automatic measurement radiographic analysis, is the most effective way to determine the NSA because it has low radiation doses, low costs, high accuracy, and a simple interface. Technology using available radiographic images provide much less radiation risk than computed tomography (CT) with a high accuracy rate of more than 98%. In addition, it streamlines measurement by reducing human error and variability found in manual methods and campaigns' clinical availability. Therefore, this computer imaging system advances technology in surgical planning and improves the patient's results of total hip arthroplasty (THA) with accurate NSA measurements. However, using 2D technology, the EOS 2D/3D imaging system is best suited for measuring the NSA due to its low radiation exposure, high accuracy, and user-friendly Interface. This system produces much less radiation than traditional imaging techniques such as CT and generates detailed 2D and 3D images required for accurate surgical schemes. This system's capacity to provide accurate measurement under increasing clinical efficiency makes it an excellent option for achieving the best results in THA.

Keywords: *Bone morphology; Neck–shaft angle, Femoral geometry, 3D imaging, CT scan, Dicom file*

1. Introduction

The neck–shaft angle (NSA) is a key determinant of successful, effective total hip arthroplasty (THA), a surgical procedure that is a major means of treatment for orthopedic surgery depending on how things develop [1]. A correct angle of NSA is crucial if not critical for not only achieving the best surgical results but also maintaining this biomechanical integrity in the hip joint effectively and efficiently [2]. NSA refers to the angle formed by the femoral neck and the main axis of the femur. NSA directly affects many important factors such as stability of the joint, range of movement, and whether or not hip prostheses for life are durable. In any case, loss angles can be catastrophic. NSA plays an undeniable function in THA because it protects functional orientation and positions a joint in its physiological orientation, which is a prerequisite for joint mechanics in the postsurgical course as well as a successful treatment outcome [3]. Moreover, NSA measurement errors

can lead to several serious complications such as impingement, dislocation, malalignment, abnormal mechanics, and premature wear of synthetic devices. Hence, these affected patients have several orders of magnitude greater risk of a failed endpoint; this represents increased risk that a revision surgery will be required, which will financially burden all parties [4],[5]. Accurate, reproducible measurement of NSA is a prerequisite for the long-term success of THA as a surgical procedure. How much of an improvement in patient satisfaction can be anticipated from the full functioning of the hip is paramount before and after such careful calibration and monitoring is carried out [6-8]. Recent studies have pointed out that traditional 2D X-rays play an important role in raising the precision and reliability of NSA measurements. For instance, a study based on a sample of 406 femora found an increase in the standard deviation of NSA measurements using (AP) X-rays: Men and women patients alike showed no significant difference from side to side [9]. In addition, a comparison of 2D methods and reconstructions in 3D with respect to the results revealed that although the 2D methods displayed consistent results, most of the 3D methods gave rise to an average deviation of over 5° in some cases [10]. Moreover, the effect of the situation in which images are taken was reviewed, and the results showed that the distortion caused by shots turning from standing to sideways is considerable, especially in NSA measurements [11]. They confirmed the importance of 2D X-rays for practical application and suggest that it is necessary for further detection within a clinically acceptable range of areas such as advanced imaging techniques to optimize surgical planning [12].

Recent studies have shown significant progress in the accuracy and reliability of the neck shaft. NSA is measured through automated software solutions. For example, using a study, Pointnet ++ reported an impressive average accuracy of 98.00% for automatic NSA measurement. The minimum error indicates that 2D and 3D methods produce sustained results [12]. In addition, an automatic method developed for dual-electricity X-ray absorptiometry (DXA) images showed intermethod reliability ranging from 0.57 to 0.96 compared with manual rating; this outcome suggests that automated technology may be found more than manual interobserver-rating [13]. In addition, AI-based Safelometric software was used for analysis. The evaluation showed that these automated systems provide measurement compared with traditional methods. However, some parameters demonstrate variability [14],[15]. These outcomes emphasize the ability to conclude. The automatic solution to increase clinical practice offers fast, breeding, and accurate NSA goals.

Exact NSA measurement is also required to prevent faults in the fee component status. Restoring the native NSA is important for maintaining proper joint stability, adapting to the speed range, and reducing the risk of dislocation and transplant use. Error in NSA measurements can cause anomalies in organ lengths, change joint biomechanics, and increase implant components' stress, outcomes contributing to early graft failures [16]. Research has shown that incorrect NSA can increase the risk of artificial effects, a condition that often leads to disadvantages, limited movement, and capacity for prosthetic disorders [17]. In addition, incorrect NSA restoration may promote increased polyethylene lining wear in the acetabular component, which may lose decay, one of the leading causes of audit surgery in THA [18].

Integrating 3D imaging into regular clinical exercise-integrating terraces and automated software represents a significant jump in NSA assessment. For example, in modern THA, where accuracy and reliability are of the most importance, the ability to correct and copy the NSA is important for reducing complications and improving the patient's results over a long time [1٧]. Growing evidence supporting the use of these advanced techniques emphasized the value of increasing the general quality of the care of patients who underwent hip replacement surgery [1٩]. These coming sessions are repeatedly discovering a few questions. People generally use thermal techniques to assess measurement accuracy. NSA is now a means of advanced imaging combining methods such as computed tomography (CT) and artificial intelligence (AI) analysis. How comparable is manual measurement of NSA with automatic methods? What does this mean for healthcare decisions because some method is impractical for large-scale adoption? How do age and gender affect the NSA measurements, and why is this of paramount importance in pediatric hip assessment? What effect does the experience of the observer have on the consistency of NSA measurements? Moreover, what effect do training and learning new techniques carry in different radiological practices over different levels of accuracy for each person who actually measures the results? In what way can standardized protocols and advanced imaging techniques increase the reliability of NSA assessment throughout various patient populations?

2. Data Collection Strategies for Hip Anatomy Studies

This research is a comparative evaluation of neck shaft attitude dimension methods. To ensure a complete evaluation, this study employed a systematic approach across 24 methodologies covering 54 individuals (48 men and 6 females) with a median age of 34 years and a BMI of 26 kg/m², who underwent CT imaging using Toshiba Aquilion or GE Discovery scanners for anatomical exams related to femoroacetabular impingement (FAI). This systematic records was collected to facilitate the assessment of various measurement strategies. Additionally, it enabled the integration of diverse imaging modalities and player demographics and enhanced the robustness of the findings. Additional research protected the evaluation of 30 pelvic radiographs from the World COACH consortium, 300 pelvic radiographs for neck–shaft angle measurements, and 533 cadaveric specimens from the Hamann–Todd Osteological Collection to assess hip morphology. Biplanar pics were obtained from 2341 EOS examinations on youngsters aged 4 to 16, while bilateral CT scans were taken from 50 University Medical Center Utrecht subjects for alignment checks. The examination additionally involved DXA scans from 4625 contributors and retrospective reviews of patients with suspected FAI using 3D CT and 3D magnetic resonance imaging (MRI). Cadaveric specimens from the New Mexico Decedent Image Database were analyzed for interobserver reliability, and a comprehensive review of patients aged four months to 19 years was conducted to evaluate hip growth. Furthermore, pelvic CT scans from 100 other patients also unrelated to hip symptoms were examined in terms of morphological measurements. Of these, demographic data were collected from trauma-related CT scans, and reliability was assessed. The studies underline one trend: Strict data-collection methods are used to ensure an accurate picture of hip morphology among different ethnic backgrounds and with varying medical workups for distinct individual cases in specific instances that are all distinct from one another.

Inclusion criteria included the measurement of the NSA on a plain conventional method, CT scan, or MRI. The number of analyzed patients, mean NSA, and applied technique for NSA measurement were disclosed. Extracted data from publications included names of authors, year of publication, number of patients, NSA values across all subjects and subgroups regarding age, gender, type of imaging software used, and intra- and inter-observer intraclass correlation coefficients (ICC).

Exclusion criteria encompassed previous surgery on the femur or hip, presence of a hip prosthesis as well as reviewing articles, editorials, comments, and letters to editors without original data, nonhuman subjects, history of pelvic fracture on the same or opposite side, and languages other than English.

Finally, the evaluation measurement of NSA depends on ICC values and its effect on clinical applications, as illustrated in Figure 1.

2.1. Measurements Neck–Shaft Angle in Two Dimensions

In a 2D assessment, NSA is usually measured by using radiographic methods. NSA is determined by a specific identification of anatomical landmarks portrayed on frontal radiographs by several different methods. Different approaches can be used to determine NSA. One way to determine NSA is by drawing lines to define the femoral neck and shaft axis. This exact technique is used to find the NSA. These lines are used in the next step of the calculation. NSA is primarily evaluated on plain radiographs, where the relationship between femoral neck and shaft is assessed in the frontal plane. This method is commonly used in clinical settings because of its availability. This method enables quick evaluations, which is a great benefit.

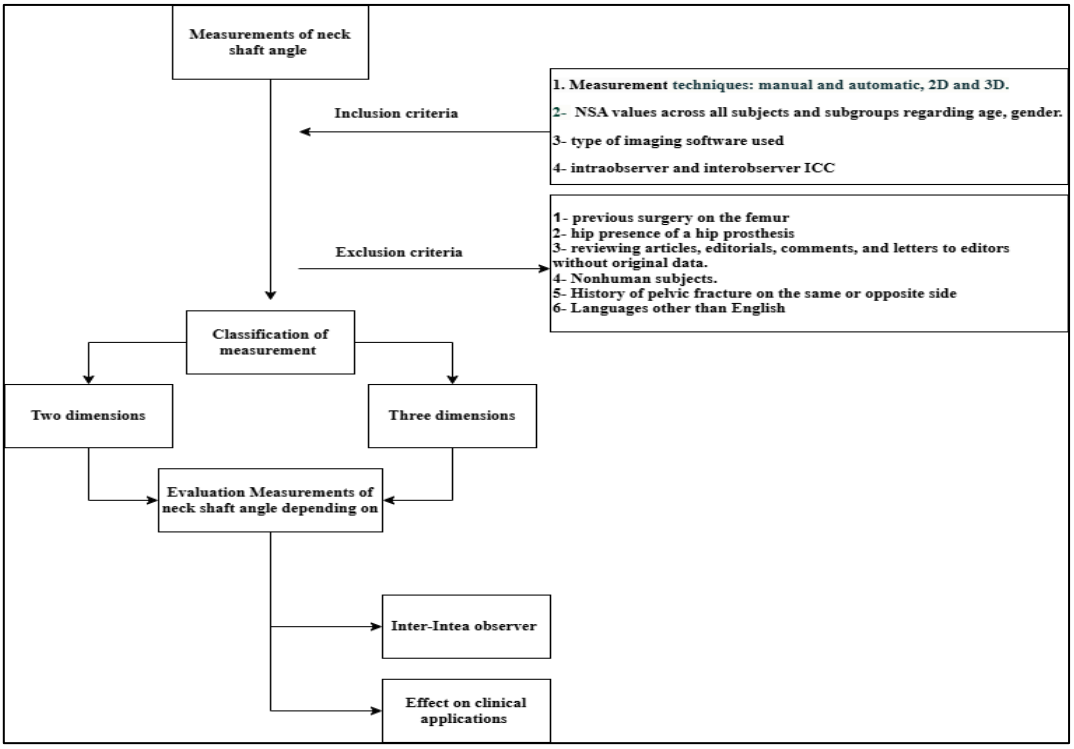

Fig. 1 Flowchart of Classification and Evaluation for Neck–Shaft Angle Measurement

2.1.1. Measuring Femoral Neck–Shaft Angle Using Computed Tomography Imaging

Bulat et al,[٢0]. measured femoral neck shaft angle (FNSA) by using CT imaging and then analyzed using OsiriX software. Figure 2 illustrates the methodology for measuring the femoral NSA in a coronal view of a CT scan, explicitly depicting the right femur of a 10-year-old boy with right hip instability. Femoral NSA is defined by the intersection of two lines: one bisecting the long axis of the femoral shaft and the other aligned with the axis of the femoral neck, which extends through the center of the femoral head. The NSA was explicitly measured in the cohort of individuals with Down syndrome, and the average value reported was 133.5° (±6.5°). The measurements' ICC demonstrated a high-reliability level, and values ranged from 0.81 to 0.99, which indicate a high level of agreement between independent raters when evaluating this parameter; the two-way mixed-effect model was used to calculate ICC in SPSS software .

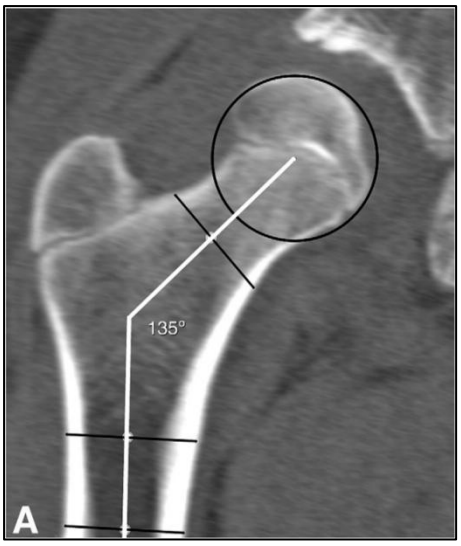

Fig. 2. Coronal computed tomography imaging methodology for evaluating femoral neck–shaft angle [20]

2.1.2. Anteroposterior Imaging Technique for Accurate Measurement of True Neck–Shaft Angle in Cadaveric Femora

Tu et al,[21]. illustrated the methodology for measuring true neck–shaft angle (tNSA), as shown in Figure 3. The measurement uses an AP imaging technique, where a lift is placed under the femoral

condyles to ensure that the femoral neck is parallel to the imaging table and effectively neutralizes any femoral version. The center of the femoral head is identified using a template with concentric circles to facilitate the precise drawing of the head–neck line and proximal femoral anatomical axis. The point where these lines intersect is the angle that represents the tNSA. According to the study, intraobserver ICC was 0.81 and inter-observer ICC was 0.82; these results demonstrate very good reliability of these measurements. Standardized digital imaging methods were used to calculate the NSA, and SPSS version 22.0 was used for statistical analyses to explore inter-relator reliability and hip osteoarthritis-related correlations .

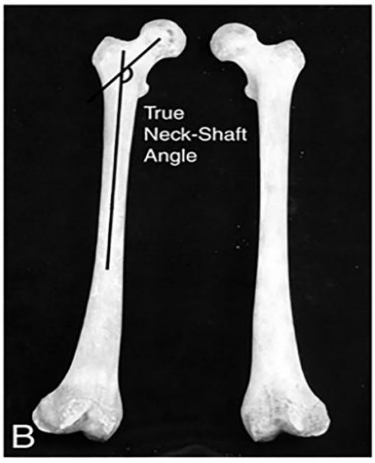

Fig. 3. Methodology for measuring true neck–shaft angle using anteroposterior imaging [21]

2.1.3. Manual Measurement Techniques for Assessing Neck–Shaft Angle in Pelvic Radiographs

F. Boel et al,[22]. assessed the reproducibility and agreement between a manual method and an automated method for morphological assessment of the hip, specifically, NSA, and other parameters. For manual measurements, the authors reported intraobserver ICCs ranging from 0.26 to 0.95 and interobserver ICCs ranging from 0.43 to 0.95 with strong reliability, specifically for the lateral center edge angle. Figure 4 shows NSA and the anatomical landmarks for its measurement. Methods: Data on segmented images of CT scans were obtained with Bonefinder® software making automated measurements that are as reliable as manual measurements to validate it for clinical setting usage. Study findings were further validated using two additional computerized mixed-effect models to analyze these measurements in R statistical software .

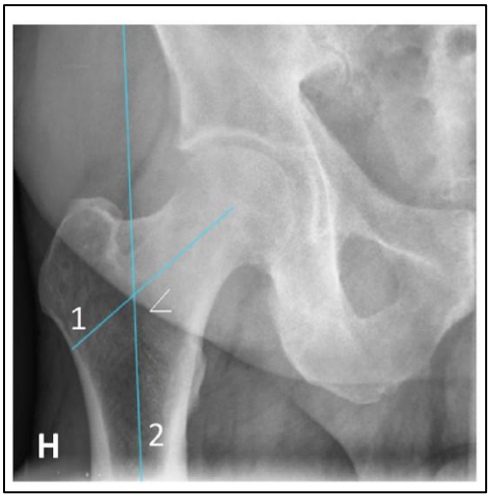

Fig. 4. Neck–shaft angle–the angle between the femoral head-neck axis (line 1) and the longitudinal axis of the femoral shaft (line 2) [22]

2.1.4. Automated Measurement of Neck–Shaft Angle Using AI-Powered Radiographic Analysis

Schwarz et al,[6]. produced output for one assessment. All pelvic radiographs were scored by the AI software (HIPPO); additional information is available in Figure 5. Figure 5 shows a pelvic radiograph with superimposed relevant measurements and more explicitly, the NSA and additional noteworthy parameters. This figure shows how the AI software automates the measurements by overlaying the calculated angles on the radiograph. The intraobserver ICC for the NSA was 0.78 (good agreement), and the interobserver ICC was 0.71 (moderate agreement). The NSA was determined by the mediCAD® v6.0 software by three orthopedic surgeons blinded to one another's measurements and to the AI outputs to eliminate any bias in the assessment of this crucial metric, and the NSA was analyzed using the ICC in the two-way mixed model in SPSS software .

Fig. 5. Automated evaluation of neck–shaft angle using AI in pelvic radiographs [6]

2.1.5. Effect of age and gender on neck–shaft angle measurements using 2D radiographic imaging

Ding et al,[23]. used 2D radiographic imaging to measure NSAs and employed MedSynapse 5.0.1.3 software (PACS) for data analysis. NSA measures decreased significantly from 4 months to 14 years of age, but the changes were hardly noticeable between 15 and 19 years. The ICC of the two observers for NSA measurements was 0.84, indicating that their assessment technique is highly reliable. The study used statistical software SPSS 25.0 for data management and analysis. In the research papers of Figures 6 and 7, age and gender affected the NSA measurements. Figure 6 shows the computed age-related changes in NSA among the pediatric patients: NSA dropped sharply from 4 months to 14 years of age. Data show that as children grew, their NSA became narrower. This outcome may also suggest that the NSA settles down after 14 years of age—NSA is set into a mature state by late adolescence. Figure 7 illustrates the differences in NSA measurements between male and female pediatric patients at different ages. Male children presented with a higher average NSA than female children at some ages—4, 8, and may happen at 12 years. This outcome may also indicate that these differences diminish or become insignificant in later adolescence, which suggests that hormonal and developmental factors influence the NSA during early growth phases .

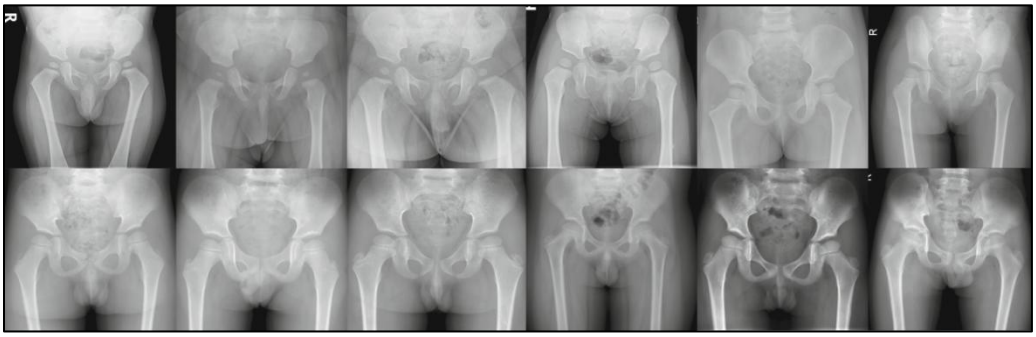

Fig. 6. Hip radiographs for children age between four months to 9 years [23]

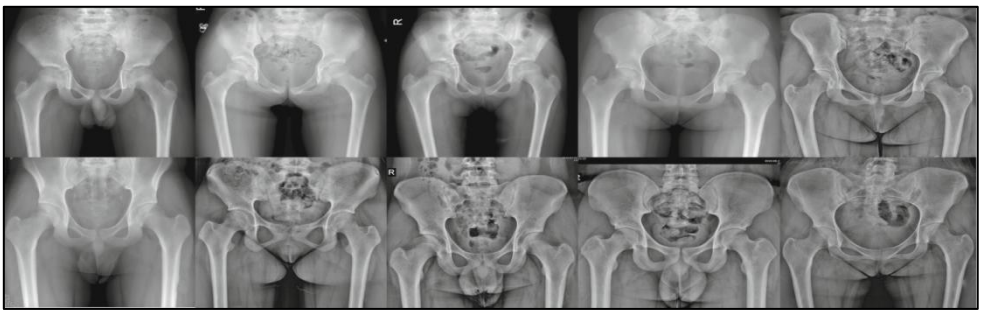

Fig. 7. In Hip radiographs of children aged 10–19 [23]

2.1.6. Assessment of Femoral Neck–Shaft Angle Using Traditional 2D Measurement Techniques

Zhao et al,[24]. employed a 2D measurement technique to evaluate the femur's NSA, concentrating on conventional imaging methods. Figure 8 illustrates the relationship between two key axes: the femoral neck axis (NC) and the shaft axis (EO). The EO connects the entry point (E) and the exit point (O) of the femoral canal centerline. The NSA is defined as the angle of intersection between these axes in 3D and the 2D coronal plane, whose 2D value is 127.06°. The reliability of such measurement was assessed using ICC, which gave a magnificent range of consistency values between 0.972 and 0.996 for intraobserver evaluations; this value shows good agreement in measurements between various observers using paired sample T-test SPSS software .

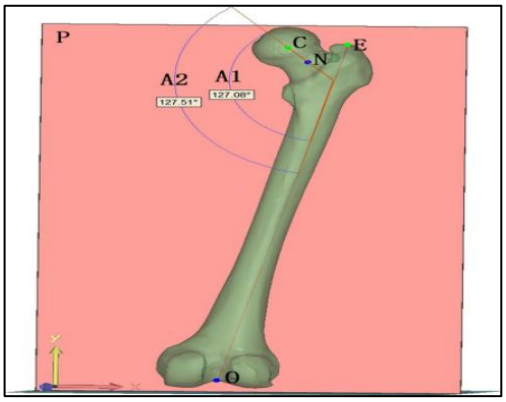

Fig. 8. Intersection of femoral neck and shaft axes: determining the neck–shaft angle [24]

2.1.7. Calculating the femoral neck–shaft angle: The method of modified neck–shaft angle

Boese et al,[25]. proposed a method that appraises fNSA and called it modified neck–shaft angle (mNSA), which is influenced by rotation in the hip to a lesser extent than the typical NSA. mNSA is achieved by purchasing scans through a CT scan, namely, the series of reconstructions CT scout view simulating nonstandardized radiographs, anterior pelvic plane view, and femoral neck plane view, an approach eliminating rotational influence. Measurements were made using software from a picture archiving and communication system (PACS) and later analyzed using IBM SPSS Statistics and Microsoft Excel. The picture shows all the measurement techniques to define the fNSA and mNSA. In Figure 9(a), traditional NSA, which uses knowledge of the center of rotation for the femoral head and the femoral neck's waist to establish the femoral neck axis (FNA), is demonstrated. Two circles must be drawn around the subtrochanteric region to establish the femur's long axis (FLA) within this method. Then, the neutral angle formed between the FLA and FNA is derived. By contrast, the mNSA method presented in Figure 9(b) helps simplify the procedure because an explicitly defined FNA need not be involved. From the FLA, a perpendicular line is constructed and intersects at the location of the minor trochanter. Then, this intersection is connected to the center of rotation, where the angle between this line and the FLA is measured. The average mNSA was 147.0° with a 95% confidence interval of 146.7°–147.4°. Its excellent intra- and inter-rater reliability are shown by the mNSA measurements for one observer and two independent observers. The measurements featured impressive ICC scores of 0.983 and 0.949. This outcome suggests high consistency across different observers and measurements. Statistical analyses were conducted using IBM SPSS Statistics for Macintosh version 22.0 and Microsoft Excel 2008. The mNSA method uses very defined anatomical landmarks, namely, the femoral shaft axis and a modified FNA defined by the center of the femoral head and the apex of the minor trochanter, to minimize rotational errors in the measurements. This outcome guarantees that the measurements are repeatable regardless of the position of the hip. Disambiguating CT imaging that provides a 3D view of the bone structures in the mNSA method clears projectional errors usually found in traditional radiography. Moreover, it provides a simulated radiographic view for different hip positions and removes external rotational influence on measurements. Using a standardized measurement protocol also plays a vital role in increasing reliability and enables training the observer to recognize these landmarks accurately; thus, it is beneficial for clinicians with minimal experience .

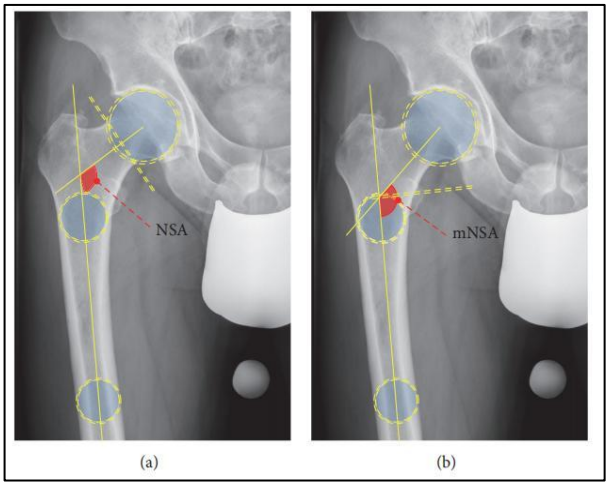

Fig. 9. Schematic of the measurement for (a) neck–shaft angle and (b) modified neck–shaft angle

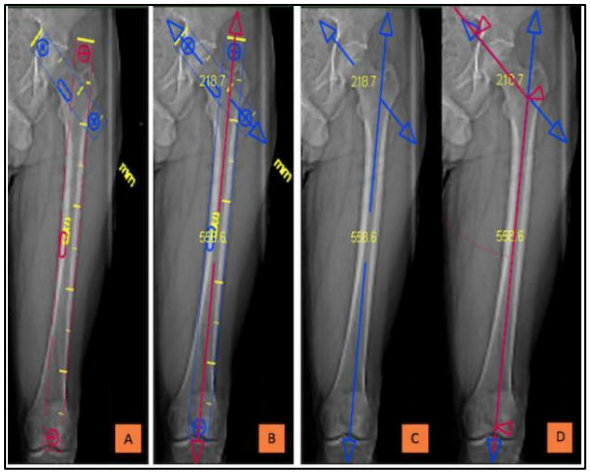

Fig. 10. Step-by-step process for assessing neck–shaft angle in femurs [26]

2.1.8. Measuring the Neck–Shaft Angle Using Computed Tomography Scout Images

Altubasi et al,[26]. for measuring the NSA using CT scout images explicitly employed SliceOmatic software for analysis. The NSA's measurement using CT scout images is illustrated in several steps. First, rulers are placed along the femoral neck and shaft to establish reference lines, and arrows are aligned at the center of these rulers. Finally, a protractor is used to calculate the angle formed between these two axes and to provide a precise angle measurement essential for evaluating hip conditions, as illustrated in Figure 10. The average NSA was 131.3° across 100 measurements, and inter- and intra-rater reliability were assessed using ICCs of 0.726 and 0.630, respectively. These values indicate good reliability for the NSA measurements and suggest that the CT scout view method is a promising alternative for assessing hip anatomy in clinical settings; the method used to calculate ICC is the two-way random model by SPSS software .

2.1.9. Measuring Femoral Neck–Shaft Angle Using Multiplanar Reconstruction

Clinger et al,[27]. used RadiAnt DICOM Viewer software to measure the femoral neck–shaft angle (FNSA) from thin-cut CT scans of cadaveric specimens using multiplanar reconstruction (MPR). FNSA is the angle between the femoral neck and shaft, and AV is the acetabulum orientation. To ensure accuracy, three independent observers aligned the femur longitudinal axis with imaging planes. The average FNA was 130.1° (115.7°–144.7°). The ICCs for FNA were 0.61 (good reliability) and 0.88 (excellent reliability), which indicate measurement consistency across observers. Figure 11 shows the methodology for measuring the FNA using MPR from thin-cut CT scans. The method consists of three key components: Figure 11A illustrates the identification of the longitudinal axis of the femur on sagittal imaging, which is crucial for accurate alignment during measurement. Figure 11B shows aligning the axial plane parallel to the femoral neck, which ensures a true anterior-posterior view is obtained on coronal imaging. Figure 11C demonstrates the actual measurement of FNA, where lines are drawn parallel through the midline of the femoral neck and aligned with the longitudinal axis of the femoral shaft. This systematic approach allows precise, reliable FNA measurements essential for hip anatomy and pathology; ICC was calculated using the ANOVA method in RStudio software .

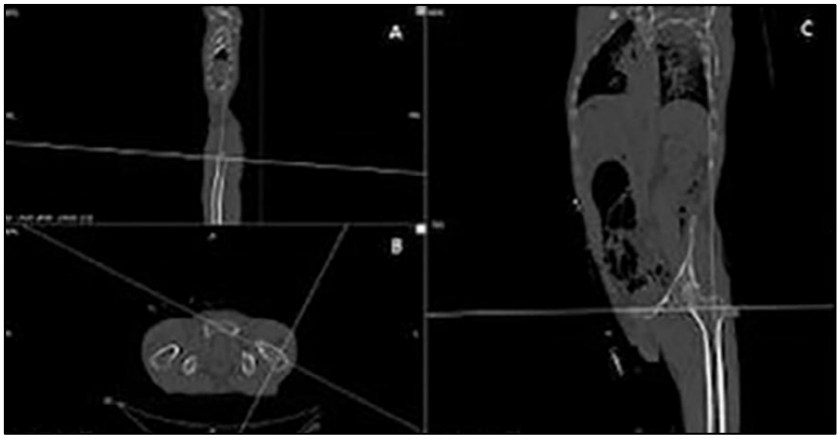

Fig. 11. Methodology for measuring femoral neck–shaft angle using multiplanar reconstruction [27]

2.1.10. Assessing Neck–Shaft Angle Using a 2D Manual Measurement Technique

Hermanson et al,[28]. calculated the NSA and head shaft angle (HSA) in children with cerebral palsy (CP) using a 2D manual measurement technique based on standard AP radiographs. Figure 12 illustrates the methodology for measuring the HSA in children with CP using three key lines: The first line is drawn through the inferior and superior margins of the femoral epiphysis to establish a reference point for the femoral head. The second line is drawn perpendicular to the first line to serve as a baseline for comparison. The third line is traced along the femur's midshaft. The angle between the perpendicular line to the femoral head and the femoral shaft represents the HSA. Inter-rater reliability for the HSA was 0.92 (95% CI 0.87–0.96), and intra-rater reliability values were 0.98, 0.94, and 0.98 for each rater, which indicate strong consistency in measurements across raters and time. Two-way random method in SPSS was used to calculate ICC .

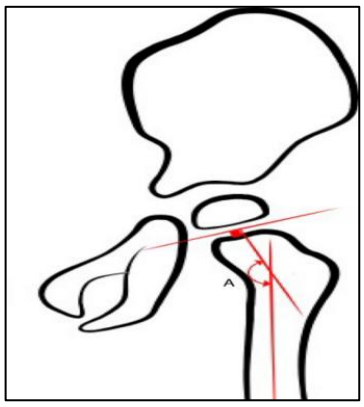

Fig. 12. Measurement technique for head shaft angle in pediatric patients [28]

2.1.11. Reference Points Marked on Anteroposterior Radiograph for Measuring Neck–Shaft Angle of the Proximal Femur

Ahmed et al,[29].'s study on measuring the femoral neck–shaft angle using CT in healthy Egyptian adults employed software for image analysis and reconstruction. Figure 13 shows the measurement protocol for determining the femoral neck–shaft angle using a simulated AP radiograph of the right proximal femur. The primary reference points are marked: M represents the center of the femoral head, A is where the circular template intersects the lateral cortex of the femoral neck, and B intersects the medial cortex. The FNA is a line perpendicular to segment AB that passes through point M. The FLA, which is necessary for calculating the NSA as the angle between the FNA and the FLA, is also shown. This figure demonstrates the anatomical landmarks and methodological steps required for accurate NSA measurement. The mean NSA was 129.46° ± 5.06° in the simulated anterior pelvic plane and 127.73° ± 4.93° in the rotation-corrected coronal reconstruction femoral neck plane. The ICC for inter-rater reliability was high at 0.93, which indicated excellent agreement between measurements taken by different observers. Intrarater reliability was also strong at 0.87, which confirmed consistent measurements by the same observer; the ANOVA method in SPSS software was used to calculate ICC .

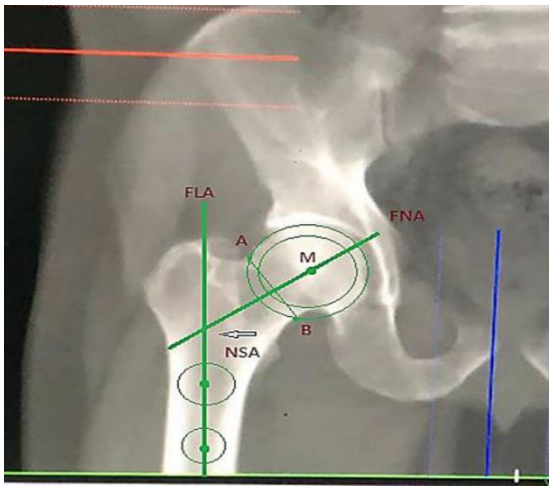

Fig. 13. Visual guide to measuring femoral neck–shaft angle using computed tomography imaging [29]

2.1.12. Direct Measurement of Neck–Shaft Angle on Frontal Plane CT scans Using a 2D Tool

Ng et al,[30]. quantified the FNSA by utilizing the longitudinal axes of the femoral neck and shaft on the frontal plane of CT scans, as illustrated in Figure 14. The FNSA is important for determining the anatomical alignment of the hip joint in the context of FAI. FNSA is the angle formed by the longitudinal axis of the femoral neck and the longitudinal axis of the femoral shaft. In this figure, the axes illustrate how the FNSA is determined from a frontal plane view. The study demonstrated a high level of reliability for evaluating FNSA with 2D CT scans and showed intraobserver correlation coefficients (ICCs) between 0.88 and 0.97. A two-way mixed model was employed to calculate ICC in SPSS .

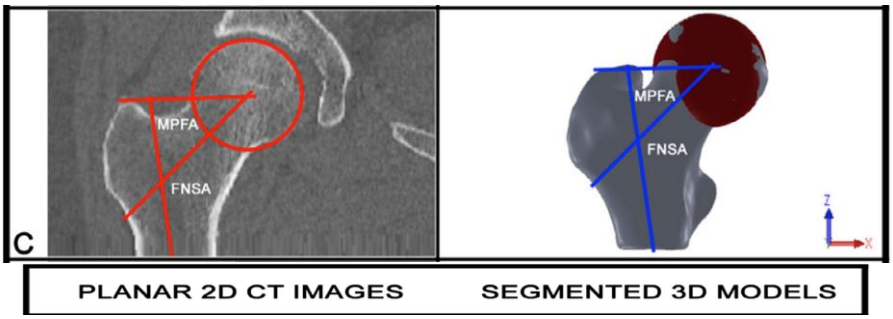

Fig. 14. Comparison of each measured anatomic parameter from computed tomography images and segmented (C) FNSA models [30]

2.1.13. Automated Measurement of Neck–Shaft Angle in Pediatric Hip Morphology Using Dual-Energy X-ray Absorptiometry Images

Boel et al,[13]. presented an automated method for determining various radiographic measurements of hip morphology, including the NSA. Figure 15 shows that the femoral neck axis is represented by a line extending from the center of the femoral head to the center of the femoral neck. The femoral shaft axis is represented by a line drawn along the femur's long axis. The intraobserver ICC for 2D NSA was 0.94, which indicated excellent reliability within a single observer's measurements, while the interobserver ICC was 0.85, which indicated strong agreement between observers. Automated calculations were carried out using BoneFinder® software for landmark identification and Python v3.9.13 to implement the measurement algorithms, an approach resulting in accurate, reproducible assessments in clinical and research settings. ICC was calculated using a two-way mixed effect model in R statistical software .

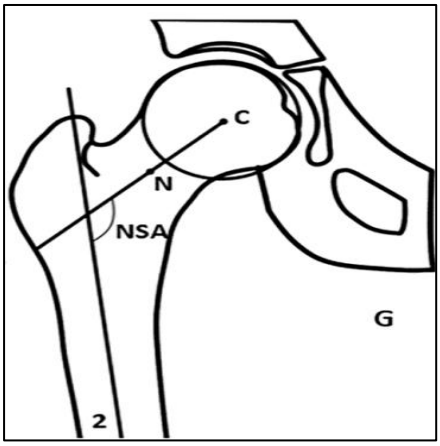

Fig. 15. Neck–shaft angle: the angle between the femoral neck axis (line 1) and the femoral shaft axis (line 2) [13]

2.1.14. Standardized 2D Radiographic Measurement Protocol for Neck–Shaft Angle Assessment in Pediatric Populations

Foxcroft et al,[31]. used full-length AP radiographs to establish normative values for lower limb alignment in South African children aged 5 to 18. Figure 16 illustrates the average combined lower limb alignment measurements in South African children, with emphasis on medial neck–shaft angle (MNSA) stability across age groups. The data reflect that the MNSA did not exhibit significant variation as children grew, an outcome suggesting that these values can serve as reliable normative reference points for this demographic. The intraobserver ICC for the MNSA was 0.88, and the interobserver ICC was higher than 0.90, showing high measurement reliability. The NSA was calculated using standardized methods described by Paley et al., and measurements were taken using Philips IntelliSpace PACS software. The NSA was analyzed using Statistica and Stata software for statistical significance and reliability assessments .

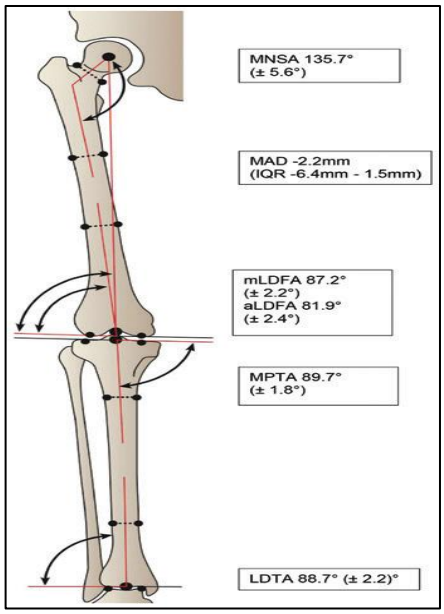

Fig. 16. neck shaft angle in South African children. Data is expressed as mean (± standard deviation) [31].

2.1.15. Standardized Measurement Protocol for Neck–Shaft Angle Using Anteroposterior Pelvic Radiographs

Haddad et al,[11]. investigated the NSA in standing and supine radiographs to determine its reliability as a measurement template for hip pathologies. Figure 17 shows the measurement technique for NSA on an upright pelvis plain radiograph. This diagram highlights key anatomical points: HC represents the femoral head center, and NC represents the femoral neck center. The measured distance, demarcated by a line between two points, allows the more exact determination of the NSA. This measurement is essential in the orthopedic evaluation and surgical planning of hip pathologies. The intraobserver ICCs for NSA were 0.898 and 0.858, which indicate very high reliability; interobserver reliability was lower at 0.688, which shows moderate reliability. The NSA was measured geometrically on the images obtained from PACS according to a standardized protocol based on anatomical landmarks, and statistical analysis was performed by SPSS version 28.0 to assess measurement variability and reliability .

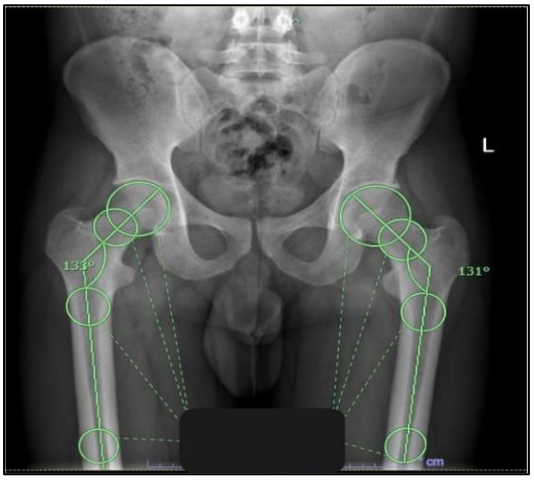

Fig. 17. Measurement technique for neck–shaft angle on an upright pelvis radiograph [11]

2.2. Measurement of Neck–Shaft Angle in Three Dimensions

The femur's anatomy can be visualized clearly with the help of 3D imaging, which is possible because of advanced software used in reconstruction. The complicated 3D spatial relationship determined by and between the femoral neck and shaft could be captured for more exact measurements relating to hip dysplasia, fracture, and other deformities. The advantages of 3D measurements are beyond accuracy and help in better surgical planning and outcomes because surgeons can visualize the anatomy. Clinicians may use these models to enhance their knowledge of individual anatomic variations to conduct a more customized surgical approach and achieve better patient care results.

2.2.1. Evaluation of Neck–Shaft Angle Measurement Utilizing 3D MRI and 3D CT Imaging Techniques

Samim et al,[32]. used 3D imaging with MRI and CT to assess femoral and acetabular morphology in patients diagnosed with FAI. The MRI was done using a Dixon 3D FLASH sequence within a 3-T scanner, an approach allowing for detailed imaging without any radiation exposure, and the 3D CT was taken with a 40-slice scanner for achieving bony assessments. The figure shows femoral neck–shaft angle (NSA) measurements using 3D volume-rendered CT and MRI images of a left hip. This figure has two panels: Panel (a) shows the NSA measurement from the 3D CT image, whereas panel (b) shows the corresponding measurement from the 3D MRI image. An ICC at 0.64 for NSA measurements indicate moderate agreement between the two imaging modalities. ICC was determined using the Shrout–Fleiss method in SPSS software. 3D CT and 3D MRI play different, but to an extent overlapping, roles in clinical imaging. Such differentiation is especially true in musculoskeletal diseases. Due to these high-resolution imaging capabilities with rapid acquisition times, most doctors favor 3D CT for better bony visualization. This approach is suitable for use in emergencies to find fractures and internal injuries quickly. It has X-ray technology, so it takes faster images but places ionizing radiation into it. The imaging is safer compared with 3D CT, yet it involves high radiographic soft tissue structures such as ligaments, cartilage, and muscles .

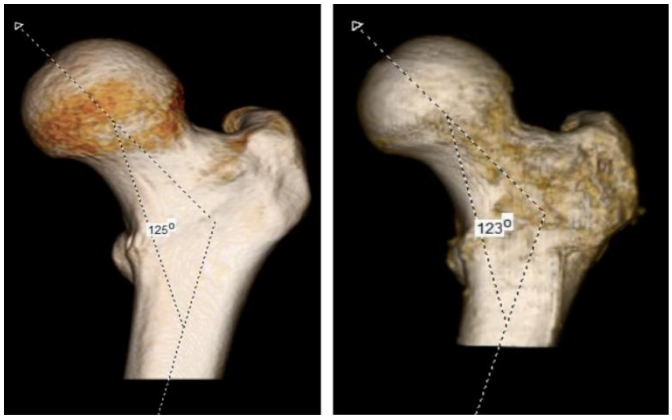

Fig. 18. Measurement of the femoral neck–shaft angle: Left image: 3D volume rendered CT image and Right image: MRI image of the same patient's left hip [32]

2.2.2. Assessing the Neck–Shaft Angle of the Femur: A 3D Measurement Technique Using Traditional Imaging Methods

This investigation applies the 3D measuring method created by Zhao et al,[24]. to determine a specific relationship between the femoral neck axis (NC) and the shaft axis. The shaft axis is constructed on a femoral canal's entrance (E) and exit (O) points. Angle NS is represented in Figure 8 concerning the intersection of these axes measured from 3D space and the 2D coronal plane. Using software Mimics and 3-Matic (Materialise, Belgium), researchers developed 3D models of the involved femur and femoral canal in CT scans and estimated anatomical parameters behind the femoral antegrade intramedullary nailing exactly. The NSA was determined by the intersection between the axes formed by a 3D representation of the femoral neck and shaft. The NSA was 127.08°. This measurement's reliability was then assessed using ICCs. The results showed excellent intraobserver reliability of the generalized ICC, mostly estimated to be in the range of 0.972–0.996, and indicate some consistent measurements across observers and trials analyzed by a paired sample T-test within SPSS.

2.2.3. Automated Measurement of Neck–Shaft Angle Using Radiographs

In contrast to the existing methodology, the present method from Park et al,[33]. for determining NSA is an automated method that uses a single or dual radiograph to extract measurements for femoral morphology, especially for subjects with CP. The development of 3D geometric femur models from CT scans, combined with principal component analysis, creates a statistical shape model. The concept of NSA is shown in Figure 19 because of its importance in inspiring clinical

thought. This value is obtained in the radiograph of the location of the femoral head's center and the femoral neck's midpoint. An angle is formed between a line joining these two points and another line that runs along the upper half of the femoral shaft. This analysis used medical image processing tools such as Mimics for 3D model generation and PACS for clinical measurements. The NSA's ICC was 0.812, which indicates high reliability compared with manual CT image measurements. A two-way mixed model was used to calculate ICC .

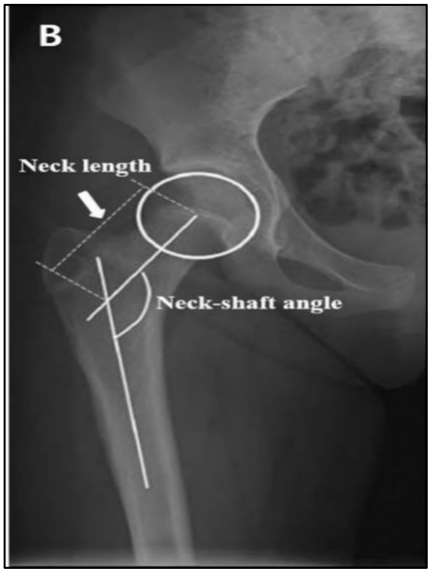

Fig. 19. Clinical parameters associated with the bowing angle of the femoral shaft on the hip lateral radiograph [33]

2.2.4. Measuring Neck–Shaft Angle Using the EOS 2-D/3-D Imaging System

The study employs the EOS 2D/3D imaging system, described by Szuper et al,[34]. which uses a biplanar slot-scanning X-ray technique to capture low-dose, high-quality images of the proximal femur and pelvis in children and adolescents. This system generates 2D images that can be reconstructed into 3D models using sterEOS software to obtain precise anatomical measurements. The NSA, which is the angle between the femoral neck axis and the proximal diaphysis axis, was measured and ranged from 130.4° to 129.3°. The intraobserver reliability of these measurements was determined using the ICC, which yielded excellent results with values of 0.95, indicating high consistency across multiple assessments. Figure 20 illustrates the NSA measured in a pediatric population using the EOS 2-D/3-D imaging system; the two-way random effect model in SPSS software was used to determine ICC.

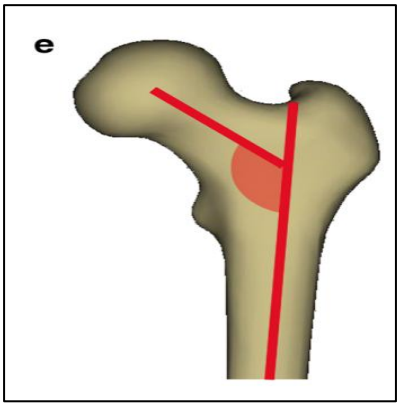

Fig. 20. Femur evaluated in the study (based on EOS 3D reconstruction images): e neck shaft (collodiaphyseal) angle [34]

2.2.5. Accurate Neck–Shaft Angle Measurement with 3D CT Image Reconstruction

The study uses Yi et al,[35].'s 3D-CT image reconstruction to measure accurately various hip anatomical parameters, including the NSA. Exact measurements were provided regardless of the patient's position, and the errors related to traditional 2D radiographs were minimized. Measurements made with Philips IntelliSpace Portal software for reconstructing images were recorded. On average, the NSA recorded was 127.0° ± 5.7° (no significant difference was noted between men and women or between sides). The ICC values ranged between 0.93 and 0.99 for intraobserver reliability, whereas those for interobserver reliability ranged between 0.91 and 0.99; these outcomes suggest high reliability for the measurements. Figure 21 shows the technique for performing the hip rotation center and femoral offset measure based on 3D CT reconstruction. The image showcases a transparent model of the hip, which allows for precise identification of key anatomical landmarks, including the teardrop center, femoral head, and relevant distances such as horizontal distance, vertical distance, and trochanteric height; the software used to determine ICC was SPSS software .

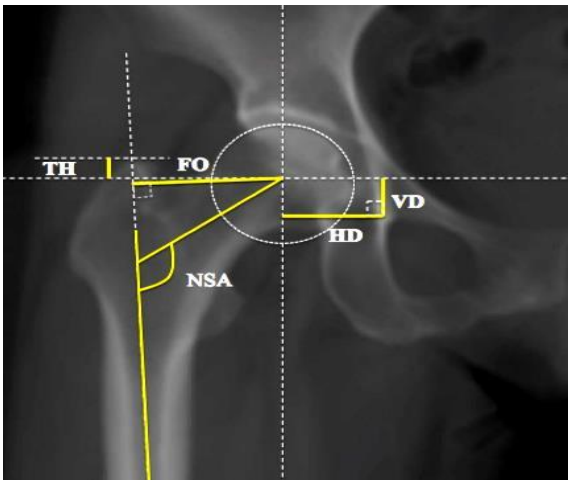

Fig. 21. Anatomical landmarks in hip morphology: A transparent model approach [35]

2.2.6. Assessment of Neck–Shaft Angle Using 3D Segmented Hip Joint Models in SolidWorks

The FNSA of the 3D segmented hip joint models was evaluated using SolidWorks program presented by Ng et al,[30]. In Figure 14 (B), the line that connects the fitted head sphere's centroid to the neck's centroid, which is the narrowest, is the longitudinal femoral neck axis. The line bisecting the distal midpoint of the diaphysis is the longitudinal axis of the femoral shaft, which extends from the piriformis fossa to the centroid center of the shaft. To estimate the FNSA, these two longitudinal axes from the 3D geometry were utilized. In evaluating FNSA, the 3D models demonstrated reliable intraobserver, interobserver, and intermethod reliability, and ICCs ranged from 0.92 to 0.99 ($p < 0.01$); the two-way mixed model was used to calculate ICC in SPSS .

2.2.7. Measuring Neck–Shaft Angle Using the EOS 2D/3D System with Bidirectional X-Ray Scanner

BurKus et al,[36]. used the EOS 2D/3D system. This bidirectional X-ray scanner takes simultaneous AP and lateral images of standing patients to perform 3D reconstruction of the spine and femur. The sterEOS software measured six proximal femoral parameters, including the NSA. Figure 22 visually represents the NSA and a comparison between different groups, such as individuals with adolescent idiopathic scoliosis (AIS) and a control group without spinal abnormalities. The illustration may include identified axes indicating the femoral neck and shaft axes, which will help clarify how the angle is measured. The NSA is important in this context because of the potential variations caused by conditions such as scoliosis, which may change hip alignment and biomechanics. Understanding these distinctions is critical for clinicians assessing treatment options and forecasting outcomes for patients with AIS. The NSA showed excellent reliability, and ICC values were greater than 0.9 based on Winer's criteria. The ANOVA method in SPSS software yielded an ICC of 0.96 for interobserver reliability and 0.93 for interobserver reliability. This method assesses the ICC by partitioning total variance into components related to differences between subjects and within groups (error). Consequently, the ICC is calculated as the variance ratio between subjects to the total variance, an approach offering valuable insights into the reliability of measurements across various conditions or raters .

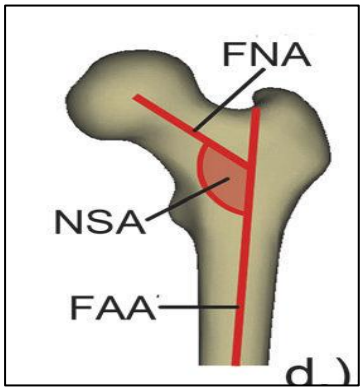

Fig. 22. Illustration of Neck Shaft Angle (NSA) Measurement in Proximal Femur Anatomy [36].

2.2.8. Measuring Neck–Shaft Angle Using InVesalius Software for 3D Reconstructions and ImageJ for Analysis

Ricciardi et al,[37]. used advanced imaging techniques and software to investigate NSA. Femoral morphology was obtained from three historical populations. CT scans of 204 femurs were examined to determine various angles, including true and apparent NSAs, using InVesalius software for 3D reconstructions and ImageJ for measurements. Figures 23A and 23B show the methodology: Figure 23 A depicts the tNSA as measured in a true AP view. NSA is defined as the angle formed by the femoral neck's axis and the shaft. A higher true NSA indicates that the femoral neck is more vertically oriented, which may have anatomical or functional implications. Figure 23B

depicts the apparent NSA measured from an apparent AP perspective. Variations in positioning or projection may cause the apparent angle to differ from the true angle. The figure displays the NSA from a specific viewpoint, which may not accurately reflect its true anatomical orientation. The tNSA values varied significantly among populations: The Neolithic population in Iran averaged 121° (±6°), the mediaeval Polish population averaged 124° (±5°), and modern Australian aborigines averaged 131° (±5°). The study also reported interclass correlation coefficients (ICC) for the measurements, which showed high reliability, values ranged from 0.85 to 0.95 across different angles, which implied consistent measurement accuracy across the samples studied; ANOVA was used to calculate ICC in R studio software .

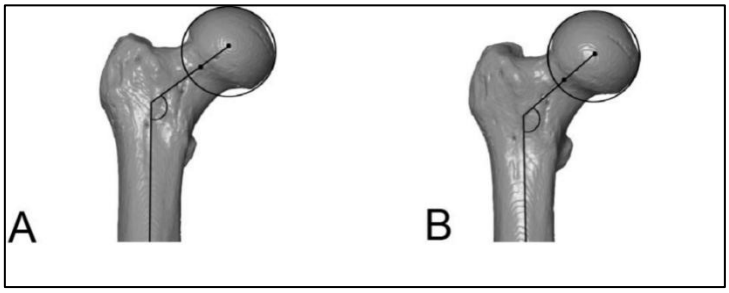

Fig. 23. Comparison of true and apparent neck–shaft angles in femoral morphology [37]

2.2.9. Automated 3D Assessment of Neck–Shaft Angle Using Computed Tomography

Kuiper et al,[38]. found that Figure 24 depicts the measurement of the NSA. The figure illustrates the anatomical landmarks used to define the NSA and shows the femoral neck and shaft axes. The angle is formed between these two axes and provides a quantitative alignment assessment. The figure emphasizes the precision of the manual method for determining this angle. The intraobserver ICC values were approximately 0.92 for the automatic method and indicated excellent reliability for repeated measurements by the same observer. The automatic method's interobserver ICC values were 0.87 and suggested good agreement between different observers' measurements. The NSA was calculated using CT scans of lower limbs, and automatic segmentation was accomplished through an AI-based workflow that utilized a neural network for bone segmentation; the two-way mixed model was used to calculate the ICC .

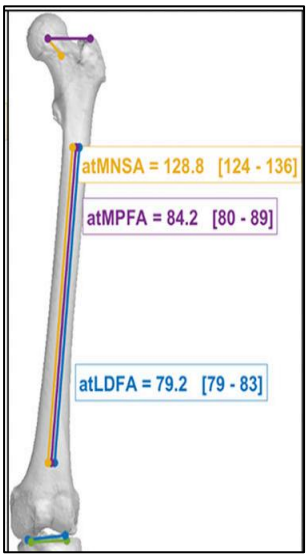

Fig. 24. images were constructed using the fully automatic method. MNSA = medial neck-shaft angle [38].

2.2.10. Manual Measurement for Accurate Assessment of Femoral Neck–Shaft Angle

The article was written by Zhe Li et al,[١2]. Figure 25 depicts the automatic measurement of the femoral NSA and highlights the steps in reconstructing the femoral model from CT data. The figure shows how the femoral point cloud is divided into three parts using the PointNet++ network: the femoral head, neck, and shaft. The figure also shows the projection plane for simulating the hip AP

radiograph in 2D and the axes for 3D measurements. Figure 26 shows a detailed methodology flowchart outlining the steps from data collection to NSA measurement and emphasizing manual and automated techniques to ensure accuracy and reliability. The intraobserver ICC for 3D manual measurement ranges from 0.76 to 0.95, while the interobserver ICC ranges from 0.58 to 0.89; specific ICC values for the 3D automatic method were not provided but are expected to be more reliable. The study utilized CT imaging collected with a GE Revolution CT scanner and employed Mimics software along with the PointNet++ network for segmentation and measurement of the NSA in 2D and 3D formats; the method two-sample student t-test used to calculate ICC in SPSS software .

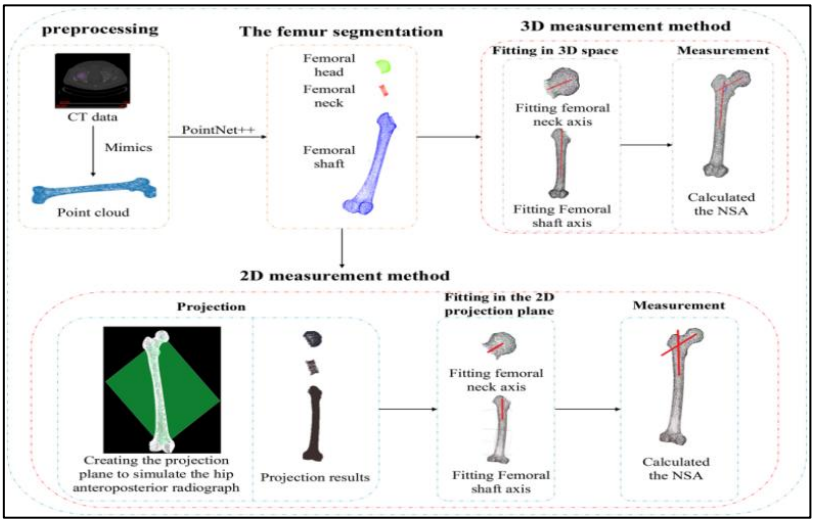

Fig. 25. Workflow of automatic measurement for femoral neck–shaft angle [١2]

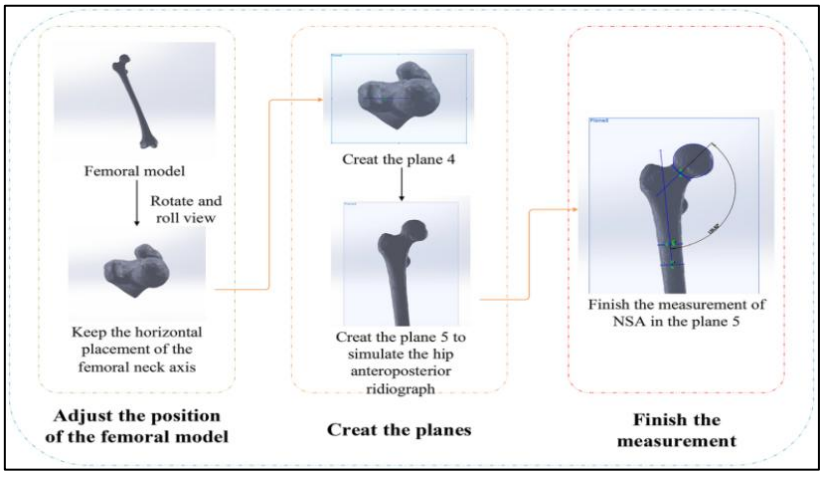

Fig. 26. Manual measurement diagram [12]

2.2.11. 3D Parametric Analysis of Neck–Shaft Angle Measurement Techniques in Femoral Version Assessment

Schmaranzer et al,[39]. evaluated how variations in proximal femoral anatomy affect femoral version measurements in young patients with hip pain. The intraobserver ICC for 3D NSA measurements was high at 0.96–0.97, indicating strong reliability when the same observer performed repeated measurements. The interobserver ICC also demonstrated excellent agreement between different observers. Figure 27 illustrates the manipulation of 3D models of the proximal femur to illustrate various NSAs. This figure displays the various NSAs the models can depict at their minimum and maximum value ranges and provides a window into the anatomical changes associated with these adjustments. These models were

systematically modified for NSA simulations ranging from 110° to 150°. CT-based NSAs were measured from scans using a Mimics v. 17.0 software approach, which allowed careful segmentation and modeling of the femur to assess its anatomical features properly. Method-related differences in femoral version measurement show marked significance and reveal clinical importance in determining the most appropriate measurement techniques in surgical planning, especially in derotational femoral osteotomy. This surgical procedure treats excessive femoral anteversion and, therefore, knee pain, hip pain, and patellofemoral instability that arise from it. Realigning the rotational position of the femur through osteotomy provides better function and relieves symptoms associated with torsional malalignment. Measurement techniques are critical because they directly affect the outcome of the surgery and the effectiveness of interventions in rectifying these deformities. ANOVA calculated statistical analysis (ICC) in GraphPad Prism .

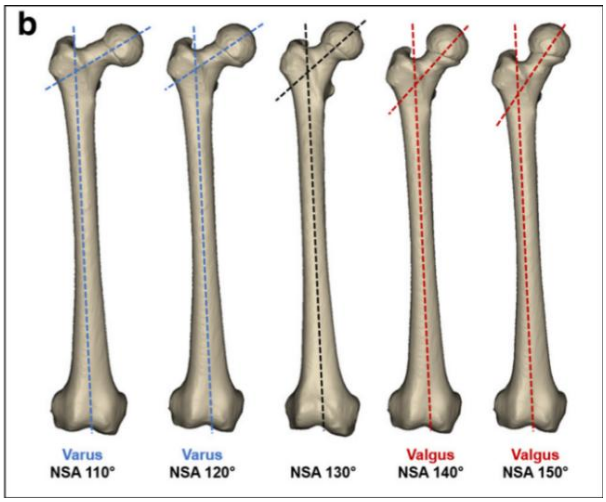

Fig. 27. 3D manipulation of femoral models to simulate variations in neck–shaft angle [39]

3. Results and Discussion

Inter- and intra-observer reliability help ensure that the measurements and examinations through multiple raters or observers are correct or regular. Intraobserver reliability refers to the similarity of repeated measures taken by using one observer at unique times and emphasizes the critical aspects of repeatable, strong results through the years via a single rater. High interobserver reliability proves that no external factor would significantly affect measurements made by the observer. This aspect becomes critical in clinical studies where SC measurements influence treatment decisions and outcomes [40].

By contrast, the exactness of each observer as a constant is for interobserver reliability measures. Interobserver reliability in studies with several raters is important because it ensures the measurements are comparable with those of anyone else performing the same assessment. Interobserver reliability is usually evaluated using statistical ways such as the ICC, which assigns a numerical value to the agreement amount between raters. A high ICC returns a high agreement score, suggesting that the measurement tool or method can be replicated by various observers [41][42].

standard ICC for intra- and inter-observer control measurement correlation and agreement. Researchers may require various ICC forms for use in their studies based on study designs. The ICC value is generally less than 0.5 for poor reliability and more than 0.90 for excellent reliability [43].

Comparing methods that rely on ICC and interclass correlation indicates several differences concerning reliability and variability between studies. For instance, Szuper et al. recorded an ICC of 0.98, a value implying excellent measurement reliability with high values of ICC at 0.927 and 0.95, Ricciardi et al. and Burkus et al. bore out this reliability. Burkus et al. and Schmaranzer have given two methods, both of which obtained high ICC values of 0.92 and 0.97, and showed significant differences between various classes. In other studies, ICC values differed widely from those obtained by Boel et al. (0.26–0.95), an outcome demonstrating considerable variability in reliability. Others, such as Altubasi et al., had lower ICC values (0.63), indicating reduced measurement reliability. These findings emphasize the importance of selecting appropriate methodologies based on the desired levels of measurement reliability and class differentiation, as illustrated in Table 1.

Table 1,
Intra- and Inter-class correlation for measuring the NSA and software

Author (year)	Method	Software	Intraclass correlation	Interclass correlation
Szuper et al. (2015)	Two-way random	SPSS	0.98	-
Ricciardi et al. (2021)	ANOVA	R software	0.927	0.962
Ng et al. (2016)	Two-way mixed	SPSS	0.861	0.856
			0.957	0.978
Burkus et al. (2019)	ANOVA	SPSS	0.95 (obs1)	0.92
			0.93 (obs 2)	
			0.97 (obs 3)	
Kuiper et al. (2023)	Two-way mixed	SPSS	0.9	-
			0.99	
Schwarz et al. (2023)	Two-way mixed	SPSS	0.8	0.71
Haddad (2022)	Not mentioned	SPSS	0.898	0.688
Foxcrpft et al. (2023)	Two-way mixed	Statistica and Stata	0.88	0.9
Schmaranzer (2022)	ANOVA	GraphPad Prism	0.97	0.97
Ahmed et al. (2023)	ANOVA	SPSS	0.93	0.93
Zhe Li et al. (2022)	Two-simple test	Python	0.95	0.89
Tu et al. (2021)	Not mentioned	SPSS	0.81	0.82
Boel et al. (2024)	Two-way mixed	R software	0.26–0.95	0.43–0.95
Boel et al. (2024)	Two-way mixed	R software	0.57–0.96	0.57–0.96
Yi et al. (2018)	Not mentioned	SPSS	0.93–0.99	0.91–0.99
Park et al. (2013)	Two-way mixed	Not mentioned	0.96	0.983
Bulat et al. (2017	Two-way mixed	SPSS	0.96	0.99
Ding et al. (2023)	Consistency test	SPSS	-	0.84
Zhang et al. (2015)	Paired sample test	SPSS	0.972	0.943
			0.996	0.986
Boese et al (2016)	Not mentioned	SPSS	0.949	0.944
Altubasi et al. (2020)	Two-way Random	SPSS	0.63	0.726
Clinger et al. (2023)	ANOVA	R software	-	0.61
Hermanson (2017)	Two-way Random	SPSS	0.92	0.99
Samim et al. (2018)	Shrout–Fleiss	SPSS	0.91	0.88
			0.64	0.64

Table 2,
Advantages, disadvantages, and types of neck–shaft angle measurement methods

Method	Type	Merits	Demerits
CT Imaging	2D	- Provides precise 3D visualization of femoral anatomy - Accurate NSA measurements by aligning with true anatomical planes, minimizing errors from femoral rotation - High reliability in measurements	- Requires additional postprocessing, which can be timeconsuming - Ionizing radiation exposure is a concern, especially for pediatric patients. - Not readily available in all clinical settings
3D MRI	3D	- Eliminates radiation exposure - Offers detailed imaging of bony structures - 100% agreement with 3D CT for diagnosing cam deformity	- Only 64.7% agreement for NSA measurements compared with 3D CT - Limited coverage of the femoral shaft complicates accurate NSA assessments - Inability to determine femoral shaft axis reliably in some cases
2D Radiographic Techniques	2D	- Noninvasive and accessible - High reliability with ICC of 0.84 - Enables identification of age-related changes in NSA, aiding in understanding hip development and fracture risk	- Measurement inaccuracies due to variations in positioning and image quality - Reliance on 2D images may not capture the full complexity of femoral anatomy, a situation leading to possible oversights.
Modified NSA	2D	- Reduced susceptibility to rotational effects, enhancing accuracy - High reproducibility with ICCs of 0.949 (intra-rater) and 0.944 (inter-rater)	- Increased radiation exposure due to reliance on CT scans - Complexity in measurement requiring multiple reconstructions - Substantial differences observed between

		- Provides age- and gender-dependent reference values for better diagnostics	conventional NSA and mNSA measurements complicate interpretations
EOS Imaging System	3D	- Low radiation exposure, suitable for pediatric patients - Produces high-quality, distortion-free images - Allows for weight-bearing evaluations, enhancing biomechanical understanding	- Technical limitations in modeling abnormal shapes - Longer reconstruction times for younger subjects - Exclusion of Patients with Lower Limb Abnormalities Limits Generalizability.
CT Scout Images	2D	- Reduced radiation exposure compared with full CT scans - High reliability with good ICC values - Improved accuracy through digital tools in SliceOmatic software	- Subjectivity in measurement placement can lead to variability. - Users must be proficient in software to avoid errors. - Limitations in generalizability due to strict exclusion criteria for participants
Multiplanar Reconstruction	2D	- Provides precise visualization of complex anatomical structures - Enhances measurement reliability with good interobserver consistency (ICC of 0.88 for acetabular version)	- Sensitive to pelvic rotation and femoral version complicating angle determination - Potential for human error despite training - Limited generalizability due to strict exclusion criteria
Automated Measurement Techniques	3D	- Reduces radiation exposure by using fewer radiographs - Enhances accuracy and consistency through statistical shape modeling - Good reliability (ICC of 0.812) compared with manual measurements	- High dependency on image quality and positioning - Variability in femur shapes complicates identification of anatomical landmarks. - Specific views may limit the ability to capture all morphological details.
Biplanar Radiography	2D	- Low radiation exposure compared with conventional methods - Simultaneous frontal and sagittal imaging improves assessment accuracy. - High reproducibility across examinations	- Sensitivity to patient positioning can lead to inaccuracies. - Dependence on software calibration may introduce errors. - Growth-related changes complicate interpretation in pediatric populations.
3D Segmented Models	3D	- Comprehensive measurement of femoral neck-shaft anatomy - Good intra- and inter-observer reliability (ICCs from 0.92 to 0.99)	- Manual segmentation is timeconsuming and variable. - Potential geometric distortions may affect measurements. - Fitting geometric spheres for reference points may cause differences in cam deformity cases.

Each imaging modality for NSA assessment, and their clinical relevance from Table 2, has specific advantages and limitations. CT imaging (2D) is reliable and gives a precise 3D view. CT imaging is highly reliable yet poses the risk of radiation exposure and postprocessing straining time. 3D MRI, while having no radiation exposure and a brilliant image of the bony structures, is not the best for accuracy in measuring NSA and the path of the femoral shaft axis. 2D Radiographic techniques are noninvasive and more readily available, but they suffer due to variability in positioning, which can cause inaccuracies in measurement. The mNSA method enhances accuracy but increases radiation exposure and measurement complexity. The EOS Imaging System (3D) is advantageous for its low radiation exposure and high-quality images but faces challenges in modeling abnormal shapes. CT Scout Images (2D) reduce radiation compared with full CT scans but can introduce variability due to subjective measurement placement. MPR offers precise visualization but is sensitive to pelvic rotation, while automated measurement techniques (3D) enhance accuracy but depend heavily on image quality. Biplanar radiography has some advantages because low radiation exposure imaging can be made simultaneously, although it is quite sensitive concerning patient positioning. The last method is 3D segmented models, which allow extensive measurements but consume considerable time and are likely subject to geometric distortions even after all the acquired knowledge. Therefore, each aspect has trade-offs between diagnostic accuracy, safety,

and practice applicability, which require careful selection according to clinical needs.

3.1. Potential Limitations of Study

The study conducted has advantages and disadvantages. Sample size ought to be discussed in the future. Although in some studies sufficient numbers can be argued to be obtained, they may have to be limit, which will lead to possible (negative) effects on the generalizability of the results. Moreover, studies had as few as 17 patients, and this may affect generalization into larger populations. Further, many studies were organized as retrospective studies that induced selection bias and restricted the range of patient characteristics when they were performed at single institutions. These limitations may reduce the generalizability of findings across clinical settings and patient populations. Additional barriers that can reduce the quality of the measurements were variations between imaging modalities and modifications to the instruments. Thus, the standard of results can implode. Standards have been defined to track the measurements taken, but observer variability is still a concern. Finally, the results can be influenced by variation in interpretation amongst radiologists, even when blinding is conducted. Some studies restricted their focus to individual races or age groups and did not mention other variant races. The use of imaging modalities alongside CT imaging added more questions in young patients with a propensity for radiation hazard. In a few reviews, failure to capture longer follow-up times led to long-term effects being overlooked for an intervention. More recent work should investigate these limitations before drawing conclusions. Although appropriate in this context, the situational factors meant to make up the meanings loom rather large.

3.2. Preferred Techniques Could Be Integrated into Clinical Practice and Their Potential Effect on Patient Outcomes

Advanced imaging technology such as 3D MRI using automated measurement tools can now be incorporated into routine clinical practice, where it can dramatically increase diagnosis accuracy and substantially reduce primary diagnostic radiation exposure, especially in children and other radio-sensitive populations. Workstreams may be generated over a standardized protocol for imaging work-up and education of healthcare professionals in these modalities that would lead to better preoperative planning. Together with an effective model of care that incorporates early detection as well as interventions suited to the individual patient, this study recommends lifestyle adjustments and social aids to recover resources. Although not all are optimistic for patients yet, the general forecast is good. Early diagnosis facilitates effective measures to manage it and lower the complication rate of illness. When such diagnostic data are available, the risk of clinical error or surgical complications for the physician is significantly reduced.The preoperative analysis of the structure and orientation of such soft tissues in pelvic floor walls (a novel technique referred to as “prefunctional analysis”) is redefining both traditional methods as well as greatly upgrading them in terms of not only higher but ultimately quicker returns for patients. The awareness and early management of hip dysplasia changes or FAI happening at a young age can prevent serious complications such as an aching joint and instead greatly increase long-term mobility.

3.3. Cost Considerations

As an example, 3D MRI cuts overall health care expenses even against 3D CT by reducing radiation exposure and the cost of subsequent examinations; hence, younger persons needing multiple studies are favored. Automated measurement systems promise savings through efficiencies over time, though they may have very high initial costs. Likewise, with AI tools in radiology, diligence reimbursement may arise as an issue. However, the overall improvement of diagnostic accuracy and decreased incidence of repeat imaging will have a dire effect on overall expenditure in healthcare. However, from a longer-term perspective, advancements in imaging techniques are expected to cost less than the initial expense of using them. The resulting savings may come from reduced surgical complications and hospital stays. Conventional protocols may be responsible for complications and needless therapies, which may incur upfront costs, yet they may be savings. Despite incurring high up-front costs, the EOS imaging system is more cost effective with its low radiation doses and perhaps fewer follow-up procedures. Overall, high initial costs are often associated with advanced imaging methods, but their benefits in terms of efficiencies and outcomes for the patient will often counter this.

3.4. Minimizing Radiation Exposure Through Alternative Protocols

Radiation exposure must be minimized when assessing NSA through high-technology imaging modalities and optimized protocols. These advanced imaging techniques exploit biplanar X-ray systems to obtain a patient's simultaneous frontal and lateral views for a detailed evaluation of anatomical structures with minimum distortion and radiation. These techniques could be used to assess deformations of the lower limb, where they could accurately measure lengths and angles in a weight-bearing position- this readily improvised diagnostic technique over conventional X-ray and CT scan modalities. Innovations such as the EOS imaging system that gives low-dose store radiographic images on NSA measurement without the increased radiation usually employed in single CT scans also represent a significant advance in reducing radiation. Automatically analyzed digital radiography will also reduce the need for obtaining multiple images, and careful positioning of the patient will make measurements more accurate and further diminishing radiation risk. Use of contralateral NSA as template reference minimizes additional images and ensures maximum dose restriction for keeping the patient free from any risk of ill effects due to radiation whilst not compromising the accuracy required to make good orthopedic decisions.

3.5. Specific Demanding Situations of Dimension Consistency in Medical Exercise

Achieving perfect uniformity in these clinical measurement procedures is ideal, but the process remains labor-intensive for novices.Machine-related bias and variation in measurement, arising from either the efforts of meager measuring actions or inadequate training, are mixed and become a compound effect. Faced with this variability within and between laboratories and the need to study the same type of sample across very different paths, the absence of some kind of universal protocol is a problem for many of those professional clinicians and provides for spacing out systematic optimal capturing of data and its retrieval/interpretation. The nature of the job may also have institutional limits on time and workflow that would not allow those same things to be fully documented. Moreover, behind negative incentives to judge measures may be the conviction that quality measurements are unnecessary or bothersome. Facilities must refine training programs, adjust data integration to align with healthcare delivery systems, and create a culture where measurements are seen as a key component of quality patient care.

3.6. Essential Findings: A Concise Overview of Results

- Critical Role of NSA: NSA is a critical factor for joint stability, ROM, and THA implant durability. Precise restoration of this attitude is necessary for the best surgical results and biomechanical function of the hip.
- Complications due to incorrect Measurements: Accuracy of the NSA is mandatory because inaccuracy can lead to unnecessary problems such as joint impingement, dislocation, limb length discrepancies, and multiple use of prosthetic components leading to potential revision surgeries.
- Reliability of 2D Radiographs: A strong interrater reliability for 2D RA regarding NSA measurements, particularly when taken on standing AP radiographs, is observed; however, tendencies will show larger than 5° of deviation from the 3D methodology.
- Three-Dimensional Imaging: The development of 3D imaging (CT and MRI) enables more precise and reliable measurement for neural structure, which is superior to the traditional 2D image that only provides a preoperative plan.
- Automated Measurement Methods: The automated software responses such as PointNet++ achieve high precision (up to 98%) in NSA measurement, which is a significant improvement from manual methods.
- Effects of Imaging Position: Status radiographs produce more dependable NSA measures compared with supine positions as a result of less asymmetry, an outcome emphasizing the importance of affected person positioning during imaging.
- The observer's degree of pleasure significantly affects the size conformity level; it can be improved through learning in different radiological specialties.
- Age and Gender Effect: Age and gender affect the NSA; sharing this type of variation is relevant when for accurate measurement in pediatric populations.
- Interobserver Reliability: Adequate use of standardized protocols is needed for manual measurements of NSA because these may vary significantly (ICC from 0.26 to 0.95).
- Clinical Implications of an Incorrectly Placed NSA: An incorrectly placed NSA may increase the potential risk of dislocation and a higher risk

of wear (implant), which are two key issues in any THA.

- Use of Higher Technology: More advanced imaging technique and automated software for clinical practice regarding NSA assessment could be applied to improve reliability.
- Reasoning with potential for an AI solution: If NSA measurements are presented side by side with the analysis tools being developed, then their rapidity and reproducibility would likely be shown to be at least comparable. It also indicates a shift from a very traditional form of clinical practice to a more technologically supported one.
- Hip Pathology: Heterogeneous patient studies confirm that NSA variations drive specific hip pathologies, necessitating customized treatment plans.
- Standard Protocol for Measurements: The development and use of a standard protocol for measurements across imaging modalities assessment would enhance generalizability and comparison of NSA assessment.

4. Conclusion

Measurement of the NSA may provide critical guidance for the diagnosis and treatment of hip pathologies among children and adolescents prior to surgery. With the conversion of original radiographs, the method is much less robust compared with modern CT and AI, whose accuracy is below 98%. The comparison between the automated and manual measurements indicates that the automatic technique decreases human error and variability and has a substantial clinical utility, which should be assessed further. Factors related to age, gender, lifestyle, nutrition, and activity patterns affect NSA, and they must be considered in pediatric assessment. Standardized protocols and targeted training can enhance measurement consistency across radiological practices. Advanced 3D imaging techniques, such as EOS imaging, greatly benefit surgical planning by eliciting precise linear measures of proximal FNSA with very low radiation compared with the old-fashioned methods. The computerized technique is predicted to enhance the efficiency of the measurement and will improve surgical planning and its effects on patients' present process of THA because of the assured correctness of NSA tests.

Future research on the accuracy of NSA measurement should focus on the following: The first dimension relates to the effect of various imaging conditions, for example, lightning, and calibration of equipment on measurement accuracy. The second dimension concerns the long-term clinical outcome of patients according to NSA accuracy with possible associations to recovery and complications. The third dimensions deals with the standardization of NSA confusion in clinical settings. The fourth dimension is how demographic factors such as age, gender, and ethnicity may affect the NSA measurements and the predictive value for patient outcomes. These efforts could greatly help in two domains: diagnostics and improving patient care.

Competing Interests

The authors declare no conflict of interest for authorship, research, and/or publication.

References

[1] M. Wittauer, J. Henry, G. Sánchez-Rosenberg, A. P. Lambers, C. W. Jones, and P. J. Yates, "Evaluation of reduction quality and implant positioning in intertrochanteric fracture fixation: A review of key radiographic parameters," World Journal of Orthopedics, vol. 16, no. 8, p. 106982, 2025.

[2] A. Di Martino et al., "Enhancing recovery: surgical techniques and rehabilitation strategies after direct anterior hip arthroplasty," J Orthop Traumatol, vol. 25, no. 1, p. 45, Sep. 2024, doi: 10.1186/s10195-024-00786-y.

[3] D. Tigani, L. Banci, R. Valtorta, and L. Amendola, "Hip stability parameters with dual mobility, modular dual mobility and fixed bearing in total hip arthroplasty: an analytical evaluation," BMC Musculoskelet Disord, vol. 23, no. 1, p. 373, Dec. 2022, doi: 10.1186/s12891-022-05280-2.

[4] S. P. Dasari et al., "Improved outcomes for proximal humerus fracture open reduction internal fixation augmented with a fibular allograft in elderly patients: a systematic review and meta-analysis," Journal of shoulder and elbow surgery, vol. 31, no. 4, pp. 884–894, 2022.

[5] A. Y. Bavil et al., "Simulated effects of surgical corrections on bone-implant micromotion and implant stresses in paediatric proximal femoral osteotomy," Computers in Biology and Medicine, vol. 185, p. 109544, 2025.

[6] G. M. Schwarz et al., "Can an artificial intelligence powered software reliably assess pelvic radiographs?," International Orthopaedics (SICOT), vol. 47, no. 4, pp. 945–953, Apr. 2023, doi: 10.1007/s00264-023-05722-z.

[7] A. Hosthota, M. Thandapani, and N. D. M. Ismail, "Evaluation of Neck-shaft Angle and Anteversion in Dry Femora of Adult Indian Population: A

Descriptive Analysis," Journal of Orthopedics and Joint Surgery, vol. 6, no. 2, pp. 103–108, 2024.

[8] M. Farshad, Ed., Orthopedics Must Knows. Berlin, Heidelberg: Springer Berlin Heidelberg, 2025. doi: 10.1007/978-3-662-70893-4.

[9] M. J. Rogers, T. L. King, J. Kim, T. F. Adeyemi, T. F. Higgins, and T. G. Maak, "Femoral neck shaft angle and management of proximal femur fractures: is the contralateral femur a reliable template?," Journal of orthopaedic trauma, vol. 35, no. 10, pp. 529–534, 2021.

[10] Á. T. Schlégl, V. Nyakas, D. Kovács, P. Maróti, G. Józsa, and P. Than, "Neck-shaft angle measurement in children: accuracy of the conventional radiography-based (2D) methods compared to 3D reconstructions," Scientific Reports, vol. 12, no. 1, p. 16494, 2022.

[11] B. Haddad et al., "Femoral neck shaft angle measurement on plain radiography: is standing or supine radiograph a reliable template for the contralateral femur?," BMC Musculoskelet Disord, vol. 23, no. 1, p. 1092, Dec. 2022, doi: 10.1186/s12891-022-06071-5.

[12] Z. Li, J. Yang, X. Li, K. Wang, J. Han, and P. Yang, "Comparing two different automatic methods to measure femoral neck-shaft angle based on PointNet++ network," Scientific Reports, vol. 12, no. 1, p. 12437, 2022.

[13] F. Boel et al., "Automated radiographic hip morphology measurements: an open-access method," Osteoarthritis imaging, vol. 4, no. 2, p. 100181, 2024.

[14] A. Kumar and S. Pandian, "Evaluation of accuracy and reliability of artificial intelligence-based fully automated and semi-automated cephalometric analysis software in comparison with manual cephalometric analysis," South East. Eur. J. Public Health, vol. 25, pp. 137–144, 2024.

[15] G. S. Duran, Ş. Gökmen, K. G. Topsakal, and S. Görgülü, "Evaluation of the accuracy of fully automatic cephalometric analysis software with artificial intelligence algorithm," Orthod Craniofacial Res, vol. 26, no. 3, pp. 481–490, Aug. 2023, doi: 10.1111/ocr.12633.

[16] J. Lv et al., "The notable role of telomere length maintenance in complex diseases," Biomedicines, vol. 12, no. 11, p. 2611, 2024.

[17] M. Kostewicz, G. Szczęsny, W. Tomaszewski, and P. Małdyk, "Narrative review of the mechanism of hip prosthesis dislocation and methods to reduce the risk of dislocation," Medical Science Monitor: International Medical Journal of Experimental and Clinical Research, vol. 28, pp. e935665-1, 2022.

[18] P. K. Sculco et al., "The Diagnosis and Treatment of Acetabular Bone Loss in Revision Hip Arthroplasty: An International Consensus Symposium," HSS Journal®: The Musculoskeletal Journal of Hospital for Special Surgery, vol. 18, no. 1, pp. 8–41, Feb. 2022, doi: 10.1177/15563316211034850.

[19] P. Sun et al., "Application of virtual and augmented reality technology in hip surgery: systematic review," Journal of medical Internet research, vol. 25, p. e37599, 2023.

[20] E. Bulat, D. A. Maranho, L. A. Kalish, M. B. Millis, Y.-J. Kim, and E. N. Novais, "Acetabular global insufficiency in patients with Down syndrome and hip-related symptoms: a matched-cohort study," JBJS, vol. 99, no. 20, pp. 1760–1768, 2017.

[21] L.-A. Tu, D. S. Weinberg, and R. W. Liu, "The association between femoral neck shaft angle and degenerative disease of the hip in a cadaveric model," HIP International, vol. 32, no. 5, pp. 634–640, Sep. 2022, doi: 10.1177/11207000211013029.

[22] F. Boel et al., "Reliability and agreement of manual and automated morphological radiographic hip measurements," Osteoarthritis and Cartilage Open, vol. 6, no. 3, p. 100510, 2024.

[23] K. Ding et al., "Age-related Changes with the Trabecular Bone of Ward's Triangle and Neck-shaft Angle in the Proximal Femur: A Radiographic Study," Orthop Surg, vol. 15, no. 12, pp. 3279–3287, Dec. 2023, doi: 10.1111/os.13923.

[24] J. Zhao et al., "Predicting the optimal entry point for femoral antegrade nailing using a new measurement approach," Int J CARS, vol. 10, no. 10, pp. 1557–1565, Oct. 2015, doi: 10.1007/s11548-015-1182-5.

[25] C. K. Boese et al., "The Modified Femoral Neck-Shaft Angle: Age- and Sex-Dependent Reference Values and Reliability Analysis," BioMed Research International, vol. 2016, pp. 1–7, 2016, doi: 10.1155/2016/8645027.

[26] I. Altubasi, H. Hamzeh, and M. Madi, "Measurement of neck-shaft angle using CT scout view in healthy jordanian adults-a reliability and agreement study," Journal of Advances in Medicine and Medical Research, vol. 32, no. 16, pp. 9–17, 2020.

[27] B. N. Clinger, S. Plaster, R. S. Fine, J. R. Marshall, and D. L. Richter, "Differences in CT Scan Measurements of Femoral Neck Shaft Angle and Acetabular Version Among Sex, Age, and Ethnicity from a Large Cadaveric Database," Western Journal of Orthopaedics, vol. 12, no. 1, p. 11, 2023.

[28] M. Hermanson, G. Hägglund, J. Riad, and E. Rodby-Bousquet, "Inter- and intra-rater reliability of the head-shaft angle in children with cerebral palsy," Journal of Children's Orthopaedics, vol. 11, no. 4, pp. 256–262, Aug. 2017, doi: 10.1302/1863-2548.11.170008.

[29] M. I. M. Ahmad, M. T. Bushra, A. T. Galal, and S. M. Ouies, "Computed tomography reference values estimation for femoral neck shaft angle in Egyptian healthy adults of both sexes," Egypt J Radiol Nucl Med, vol. 54, no. 1, p. 96, May 2023, doi: 10.1186/s43055-023-01040-x.

[30] K. C. G. Ng, M. Lamontagne, M. R. Labrosse, and P. E. Beaulé, "Comparison of anatomical parameters of cam femoroacetabular impingement to evaluate hip joint models segmented from CT data," Computer Methods in Biomechanics and

Biomedical Engineering: Imaging & Visualization, vol. 6, no. 3, pp. 293–302, May 2018, doi: 10.1080/21681163.2016.1216805.

[31] W. D. Foxcroft, J. du Toit, N. Ferreira, M. Thiart, A. Saini, and M. Burger, "Radiographic Assessment of Lower Limb Alignment in South African Children," Journal of Limb Lengthening & Reconstruction, vol. 9, no. 1, pp. 35–40, 2023.

[32] M. Samim et al., "3D-MRI versus 3D-CT in the evaluation of osseous anatomy in femoroacetabular impingement using Dixon 3D FLASH sequence," Skeletal Radiol, vol. 48, no. 3, pp. 429–436, Mar. 2019, doi: 10.1007/s00256-018-3049-7.

[33] N. Park, J. Lee, K. H. Sung, M. S. Park, and S. Koo, "Design and Validation of Automated Femoral Bone Morphology Measurements in Cerebral Palsy," J Digit Imaging, vol. 27, no. 2, pp. 262–269, Apr. 2014, doi: 10.1007/s10278-013-9643-2.

[34] K. Szuper, Á. T. Schlégl, E. Leidecker, C. Vermes, S. Somoskeöy, and P. Than, "Three-dimensional quantitative analysis of the proximal femur and the pelvis in children and adolescents using an upright biplanar slot-scanning X-ray system," Pediatr Radiol, vol. 45, no. 3, pp. 411–421, Mar. 2015, doi: 10.1007/s00247-014-3146-2.

[35] L. Yi et al., "Anatomical study based on 3D-CT image reconstruction of the hip rotation center and femoral offset in a Chinese population: preoperative implications in total hip arthroplasty," Surg Radiol Anat, vol. 41, no. 1, pp. 117–124, Jan. 2019, doi: 10.1007/s00276-018-2143-9.

[36] M. Burkus, Á. T. Schlégl, K. József, I. O'Sullivan, I. Márkus, and M. Tunyogi-Csapó, "Analysis of Proximal Femoral Parameters in Adolescent Idiopathic Scoliosis," Advances in Orthopedics, vol. 2019, pp. 1–7, Apr. 2019, doi: 10.1155/2019/3948595.

[37] B. F. Ricciardi, "CORR Insights®: Is Cam Morphology Found in Ancient and Medieval Populations in Addition to Modern Populations?" Clinical Orthopaedics and Related Research®, vol. 479, no. 8, pp. 1839–1841, 2021.

[38] R. J. Kuiper, P. R. Seevinck, M. A. Viergever, H. Weinans, and R. J. Sakkers, "Automatic assessment of lower-limb alignment from computed tomography," JBJS, vol. 105, no. 9, pp. 700–712, 2023.

[39] F. Schmaranzer et al., "Coxa valga and antetorta increases differences among different femoral version measurements: potential implications for derotational femoral osteotomy planning," Bone & Joint Open, vol. 3, no. 10, pp. 759–766, Oct. 2022, doi: 10.1302/2633-1462.310.BJO-2022-0102.R1.

[40] L. Quinn et al., "Interobserver variability studies in diagnostic imaging: a methodological systematic review," The British Journal of Radiology, vol. 96, no. 1148, p. 20220972, 2023.

[41] A. Mierke et al., "Intra- and inter-observer reliability of the novel vertebral bone quality score," Eur Spine J, vol. 31, no. 4, pp. 843–850, Apr. 2022, doi: 10.1007/s00586-021-07096-5.

[42] S. Picken, H. Summers, and O. Al-Dadah, "Inter- and intra-observer reliability of patellar height measurements in patients with and without patellar instability on plain radiographs and magnetic resonance imaging," Skeletal Radiol, vol. 51, no. 6, pp. 1201–1214, Jun. 2022, doi: 10.1007/s00256-021-03937-y.

[43] G. Xu et al., "Test-retest reliability of fNIRS in resting-state cortical activity and brain network assessment in stroke patients," Biomedical Optics Express, vol. 14, no. 8, pp. 4217–4236, 2023.

تحليل مقارن لتقنيات التصوير المختلفة لقياس زاوية عنق عظم الفخذ في عظم الفخذ القريب

سجاد عباس علي[1]*، احمد زيدان محمد[2]، وميض علي جاسم[3]

[1،2]قسم هندسة التصنيع المؤتمت، كلية الهندسة الخوارزمي، جامعة بغداد، بغداد، العراق

[3]مستشفى اليرموك التعليمي، وزارة الصحة، بغداد

*البريد الالكتروني: sajjad.ali2204@kecbu.uobaghdad.edu.iq

المستخلص

إن قياس زاوية عنق عظم الفخذ بدقة يُعتبر أمرًا بالغ الأهمية في المجال الطبي، حيث يؤثر بشكل مباشر على تشخيص وإدارة الحالات المرتبطة بمفصل الورك، مثل خلل التنسج الوركي والتهاب المفاصل العظمي. يمكن أن تنشأ التباينات في قياسات زاوية عنق عظم الفخذ نتيجة لاختلاف وضعية المريض أثناء التصوير، مما يبرز الحاجة إلى بروتوكولات موحدة لضمان الموثوقية. من خلال تقليل الفروقات في القياسات، يمكن لمقدمي الرعاية الصحية تحسين التخطيط الجراحي وتحقيق نتائج أفضل للمرضى. تمثل الهدف الأساسي من البحث في تحديد طريقة قياس دقيقة وموثوقة لزاوية عنق عظم الفخذ باستخدام برامج وأساليب مختلفة. وأظهرت النتائج النهائية أن الطريقة ثلاثية الأبعاد لقياس زاوية عنق عظم الفخذ، وخاصة القياس الآلي باستخدام التحليل الإشعاعي المدعوم بالذكاء الاصطناعي، هي الطريقة المفضلة لتقييم هذه الزاوية. يعود هذا التفضيل إلى انخفاض التعرض للإشعاع، والتكلفة الاقتصادية، والدقة العالية، وسهولة الاستخدام. تعتمد هذه الطريقة على الصور الإشعاعية الموجودة بالفعل، مما يقلل بشكل كبير من مخاطر الإشعاع مقارنةً بالتصوير المقطعي المحوسب مع الحفاظ على مستويات عالية من الدقة تصل إلى حوالي ٩٨%. بالإضافة إلى ذلك، تُبسط هذه الطريقة عملية القياس، مما يقلل من الأخطاء البشرية والتفاوتات المرتبطة بالأساليب اليدوية، مما يجعلها ملائمة للاستخدام في البيئات السريرية. نتيجة لذلك، تعزز هذه الطريقة الآلية التخطيط الجراحي وتحسن نتائج المرضى في عمليات استبدال مفصل الورك الكلي. من ناحية أخرى، تُعتبر طريقة (EOS) ثنائية وثلاثية الأبعاد EOS 2-D/3-D الأفضل لقياس زاوية عنق عظم الفخذ باستخدام الأسلوب ثنائي الأبعاد. تتميز هذه الطريقة بانخفاض التعرض للإشعاع ودقتها العالية وسهولة التشغيل. كما تقلل بشكل كبير من جرعات الإشعاع مقارنة بالطرق التقليدية مثل التصوير المقطعي المحوسب، وتوفر صورًا ثنائية وثلاثية الأبعاد مفصلة ضرورية للتخطيط الجراحي الدقيق. إن قدرتها على تقديم قياسات دقيقة وتعزيز الكفاءة السريرية تجعلها خيارًا مثاليًا لضمان تحقيق أفضل النتائج في عمليات استبدال مفصل الورك الكلي.